PAPER

Sonochemical synthesis of Co_3O_4 nanoparticles deposited on GO sheets and their potential application as a nanofiller in MMMs for O_2/N_2 separation

Shahnila Shah, [ID] [a] Huma Shaikh, [ID] *[a] Sarah Farrukh, [ID] [b]
Muhammad Imran Malik, [ID] [cd] Zaib un Nisa Mughal [ID] [a] and Shabana Bhagat[a]

In this study we report an environmentally friendly, facile and straightforward sonochemical synthetic strategy for a Co_3O_4/GO nanocomposite using N,N'-bis(salicylidene)ethylenediaminocobalt(II) as a precursor and graphene oxide sheets as an immobilization support for Co_3O_4 nanoparticles. The synthesis was facilitated by physical and chemical effects of cavitation bubbles. The synthesized nanocomposite was thoroughly characterized for its composition and morphology using Fourier transform infrared spectroscopy (FTIR), Energy dispersive X-ray spectroscopy (EDS), Scanning electron microscopy (SEM), UV-visible, Raman and X-ray diffraction spectroscopy (XRD), *etc.* The results show Co_3O_4 nanoparticles of 10 nm (SD 3 nm) were prepared on well exfoliated sheets of GO. The applicability of the synthesized Co_3O_4/GO nanocomposite was optimized as a nanofiller for mixed matrix membranes (MMMs) comprised of poly(2-acrylamido-2-methyl-1-propanesulfonic acid) and polyvinyl chloride. The affinity of the prepared MMMs was evaluated for the separation of O_2/N_2 gases by varying the concentration of nanofiller, *i.e.* 0.03%, 0.04%, 0.05% and 0.075% (w/v). The results display high separation performance for O_2/N_2 gases with excellent permeance (N_2 167 GPU and O_2 432 GPU at 1 bar) and O_2/N_2 selectivity of 2.58, when the MMMs were loaded with 0.05% (w/v) of Co_3O_4/GO nanocomposite.

Introduction

Recently, much attention has been drawn towards the synthesis of nanosized crystalline metal oxides with striking distinctiveness due to their vast range of applications in several fields owing to their unusual adsorptive properties, fast diffusivities, large surface areas and surface defects.[1–6] Among them, cobalt oxide nanoparticles have gained more consideration on account of their exceptional properties and promising applications in lithium-ion batteries,[7] gas sensing,[8] catalysis,[9] electrochromic devices,[10] gas separation,[11] *etc.*

The choice of synthesis method can greatly affect the size, structure and yield of the nanoparticles. The fact that the decrease in particle size leads to the size-driven phase transitions in nanoparticles has been confirmed by Emre Erdem while working on the synthesis of $CoFe_2O_4$ nanoparticles.[12]

Various synthesis protocols have been reported for the preparation of Co_3O_4 nanoparticles.[13–18] The most frequently used for this purpose are chemical reduction, calcinations or pyrolysis in the presence of appropriate metal precursors.[19] However, there are few drawbacks associated with these methods such as low efficiency, substantial time consumption, high-power indulgence, and the use of high temperature thermal treatment devices to make the product mechanically more desired and crystalline in nature.[20,21] Therefore, searching alternate novel synthetic routes by different, easier and effective manner is still prevailing and highly desired.

Sonochemistry has provided new breakthrough to the synthesis of nanomaterials especially that were prepared at high temperature and pressure conditions are now prepared at ambient conditions. The sonochemical methods are better than other methods that utilize heat, light and pressure because they are swift and simple. Moreover, they provide higher energy in short time that allows achieving better materials by modifying synthesis protocols. During sonication process of liquids their acoustic pressure becomes more negative than saturated vapor pressure that results in cavitation. A bubble can overgrow and collapse within short lifetimes (>1010 K s^{-1}). The energy released during this short process leads to rise in local temperature to ~5000 K and

[a] National Center of Excellence in Analytical Chemistry, University of Sindh, Jamshoro-76080, Pakistan. E-mail: huma.hashu@gmail.com

[b] School of Chemical and Materials Engineering (SCME), National University of Sciences & Technology, Islamabad, Pakistan

[c] H.E.J. Research Institute of Chemistry, International Centre for Chemical and Biological Sciences (ICCBS), University of Karachi, Karachi-75270, Sindh, Pakistan

[d] Third World Center for Science and Technology, International Center for Chemical and Biological Sciences (ICCBS), University of Karachi, Karachi 75270, Pakistan

pressure ~1000 bar.[22–24] The phenomenon of acoustic cavitation in solution has led to fascinating reaction routes.[25] Numerous nanoparticles and nanomaterials of transition and noble metals,[26–28] carbon and polymeric materials[29,30] and semiconductors[31] have been recently reported using sonochemical synthesis routes. Sonochemical synthesis of cobalt oxide Co_3O_4 nanoflowers and nanorods in the presence of the ionic liquid 1-ethyl-3-methylimidazolium tetrafluoroborate [EMIM][BF_4] as reaction media and morphology template has been reported.[32] Partha *et al.*[33] also reported a sonochemical synthetic route for cobalt ferrite nanoparticles. However, fewer reports are available for simple and robust routes for the synthesis of Co_3O_4 nanoparticles on suitable substrates. Carbon based supports such as carbon nanotubes, graphene and its derivatives, *etc.* have proved themselves extraordinary in context of outstanding thermal, chemical and physical properties. Among these, graphene oxide offers excellent room for the accommodation of nanoparticles with exceptional reactivity and surface area.

Graphene oxide (GO) is an atomically thin oxygenated layer comprising of oxygen functionalities on the edges and basal planes of the sheets. Due to the existence of the ionizable carboxylic (–COOH) groups on edges, it can disperse in water easily and thus has long been considered as hydrophilic. Nevertheless, the hydrophobicity of GO arises due to the occurrence of several polyaromatic patches of unoxidized graphene nanodomains on its basal plane. Therefore, GO can provide a better backbone for immobilization of different metal complexes for their improved and wider range of applications by providing the high chemical stability and specific surface area.[34] Because of the fine interlayer spacing and thinness of GO sheets (~0.6–1.2 nm), it has shown excellent separation and purification characteristics as well.[35] Thus the intercalation of particular precursors between the interlayers of GO to attain required composite can offer huge potential in the preparation and applications of different separation membranes.[36]

Herein, we report a facile and straightforward sonochemical synthetic route for Co_3O_4 nanoparticles on GO sheets using N,N'-bis(salicylidene)ethylenediaminocobalt(II) or (CoSalen) as metal precursor and GO as backbone for the deposition of Co_3O_4 NPs. Keeping in mind the efficiency of Co_3O_4NPs[37,38] for O_2/N_2 separation and applicability of graphene oxide in membrane technology, we further demonstrated the utilization of Co_3O_4/GO nanocomposite imbued as filler in the poly(vinylchloride)/poly(2-acrylamido-2-methyl-1-propanesulfonic acid) (PVC/PAMPS) blended MMMs for the separation of O_2/N_2. The fabrication of membranes were done by taking the advantage of high-performance polymers such as PVC and PAMPS owing to their superior chemical and physical properties combined with high separation performance and mechanical strength of membranes. The prepared membranes were tested to check their separation efficiency for O_2 and N_2 gases. Effect of filler (Co_3O_4/GO NC) loading on the gas permeability was also investigated. The prepared materials were thoroughly characterized using SEM, EDS, FTIR, Raman, UV-Visible spectroscopy, XRD *etc.*

Experimental

Materials

Graphite flakes, sulfuric acid, hydrochloric acid and potassium permanganate were purchased from Alfa Aesar. Poly(2-acrylamido-2-methyl-1-propanesulfonic acid) (average M_w 2 000 000, 15 wt% in H_2O), sodium nitrate, N,N'-dimethylformamide and hydrogen peroxide were procured from Sigma-Aldrich, USA. Polyvinyl chloride (PVC) ($n = 1020$) was purchased from Yakuri Pure Chemicals Co., Ltd./KYOTO Japan. Sodium sulfite, ethanol, salicylaldehyde, cobalt(II) acetate and ethylene diamine were bought from FlukaChemika, Switzerland.

Synthesis of graphene oxide

To synthesize the graphene oxide modified Hummers' method was followed.[39] For that, graphite flakes (2 g) and $NaNO_3$ (1 g) were added in 35 mL of conc. H_2SO_4 and stirred. For the safety measure this mixture had been cooled to 0 °C in an ice-bath. With continuous vigorous stirring, 6 g of $KMnO_4$ was added to the suspension carefully. The temperature of the suspension was maintained at 2 °C. After the complete addition and mixing the ice-bath was removed and the temperature was allowed to rise up to 35 ± 3 °C, where it was maintained for 30 minutes. 400 mL of DI water was then added slowly to the solution and stirred for half an hour. Finally, the suspension was treated with 5 mL of 30% H_2O_2 that resulted in the change of color indicating the reaction completion. The solution was then washed with 5% HCl and centrifuged with DI water several times until the neutral pH was obtained.

Synthesis of N,N'-bis(salicylidene)ethylenediaminocobalt(II) complex

CoSalen was synthesized through a reported method.[40] According to the procedure H_2Salen was synthesized first by taking 3 mL of ethanol (95%) in a small beaker with continuous heating and stirring, 1.4 mmol of ethylenediamine (0.10 mL) and 2.8 mmol of salicylaldehyde (0.30 mL) was added in the ethanol. After 3–4 min of agitation the solution was chilled in an ice bath and yellow precipitates of H_2Salen were collected. In the next step, 0.86 mmol of H_2Salen (0.23 g) were added in a round bottom flask and dissolved in 12 mL of degassed ethanol. In a separate flask a solution of 0.2 g of cobalt(II)acetate tetrahydrate in 1.5 mL of water was prepared that was subsequently added to the H_2Salen under continuous stirring. The reaction mixture was refluxed for 1 hour. The whole reaction was performed under N_2 stream to create an inert atmosphere. After 1 hour, the solution was cooled and brick-red precipitate of CoSalen were collected, washed with 1 mL of ice cold ethanol and dried in a desiccator. The synthesis of CoSalen was confirmed using FTIR (Fig. 3b).

Synthesis of Co_3O_4/GO nanocomposite

For the synthesis of nanocomposite, 0.01 g of GO was well dispersed into 5 mL of N,N'-dimethylformamide (DMF) *via* ultrasonication for 2 h. 0.01 g of CoSalen was then added to the

well dispersed GO and reaction was continued in ultrasonic bath for 6 h. The obtained nanocomposite was then air dried. The formation of Co_3O_4 nanoparticles finely deposited on the surface of GO sheets *via* the effect of ultrasonication of CoSalen was then confirmed by various characterization techniques.

Fabrication of mixed matrix membranes (MMMs)

The MMMs were fabricated through solution casting method. For pure membrane, 5% (w/v) polymeric solution was prepared by taking 0.5 g of PVC in 10 mL DMF. Similarly, 10% (w/v) solution of PAMPS was prepared in DMF.[41] Both polymeric solutions were then mixed and stirred for 24 h to obtain a homogenized mixture. The bubble-free solution was obtained by keeping the solution unmoved for 2 h. Resulting solution was cast into Petri dishes and dried in oven at 80 °C for 24 h. For fabrication of synthesized Co_3O_4/GO nanocomposite embedded MMM, 0.5 g of PVC was added to 7.5 mL of DMF, 1 g of PAMPS was added in another 7.5 mL of DMF, and 10 mg of nanocomposite were dispersed in 5 mL of DMF *via* 4 h of sonication at room temperature. Above-mentioned three solutions were mixed and stirred for 24 h to obtain a homogenized mixture. The resulting solution was cast into Petri dishes and dried in oven at 80 °C for 24 h. The synthesized membrane was detached from the glass surface by dipping in water. Several MMMs were prepared by varying the amount of Co_3O_4/GO nanocomposite. The MMMs were prepared by loading 0.03%, 0.04%, 0.05% and 0.075% (w/v) of Co_3O_4/GO nanocomposite following the aforesaid fabrication method.

Characterization

The surface morphology and elemental analysis of synthesized membranes and nanocomposite was studied by taking the cross-sectional images of them using SEM (JEOL JSM-6380LV) attached with EDS. For taking SEM images samples were sputter coated with a thin gold film and attached on brass plates.

For qualitative structural analysis of synthesized membranes and nanocomposite, FTIR spectrophotometer (FTS-65, Biorad) was used with resolution of 1 cm^{-1} in transmission mode and wave numbers in the range of 450 to 4000 cm^{-1}. In a pallet holder the small portion of circular shaped membrane was placed. The sample holder was then staged in the instrument and the spectra were recorded at room temperature by subtracting the background noise. Raman spectroscopy was performed for synthesized Co_3O_4/GO nanocomposite by using Thermo Scientific DXR Raman microscope with 780 nm filter.

The absorption spectrum of GO and Co_3O_4/GO nanocomposite was recorded by using Agilent-Carry 100-double beam UV-visible spectrophotometer. The spectroscopic measurements were carried out by taking the absorbance of 500 μL of 0.2% (w/v) solution of well dispersed Co_3O_4/GO nanocomposite in DMF. Shift in the absorbance were measured in the range of 200–800 nm at room temperature.
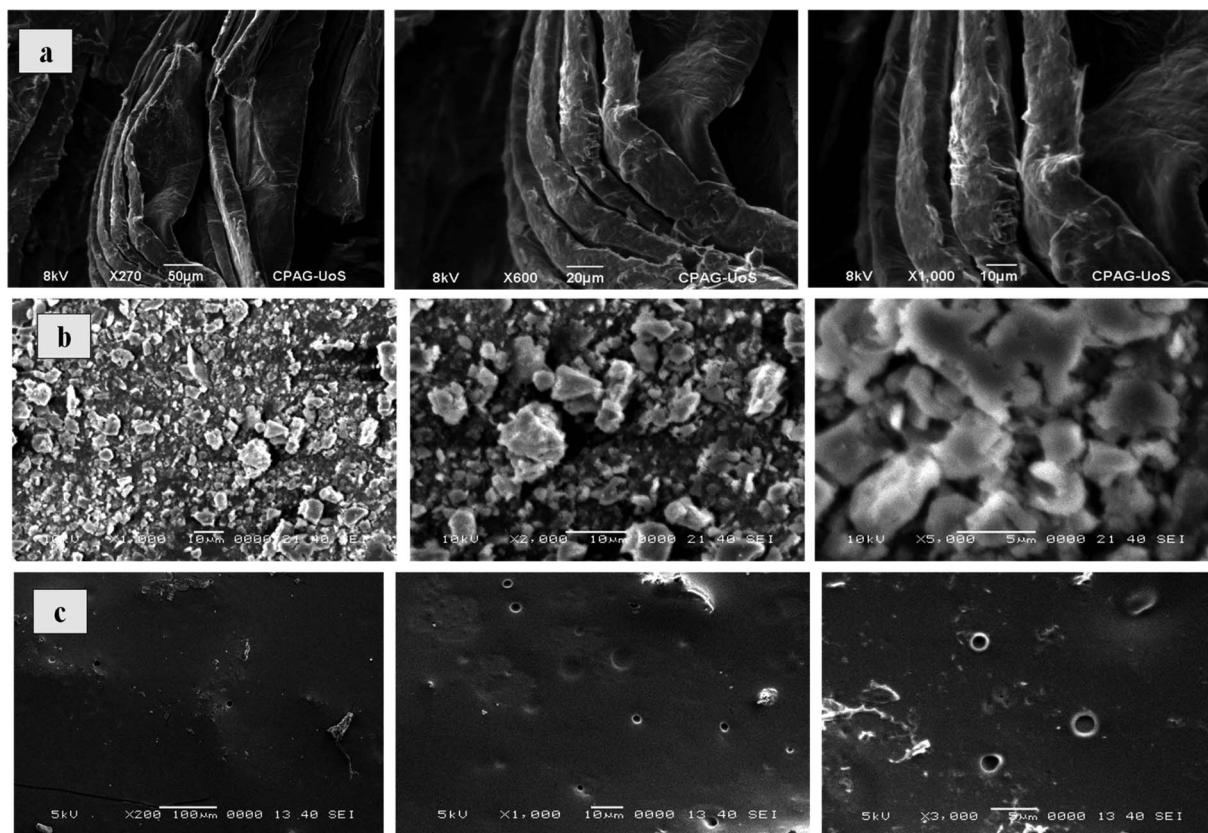

Fig. 1 SEM images of: (a) GO, (b) Co_3O_4/GO nanocomposite, (c) Co_3O_4/GO nanocomposite embedded MMM.

To examine the structural characteristics of Co_3O_4/GO nanocomposite X-ray diffraction investigation was performed. For this purpose, STOE Germany Theta–Theta diffractometer (Germany, software, WinXPoe X'Pert High Score) with Cu Kα monochromatic radiations (wavelength = 1.54 Å) was used.

Gas permeation experiments

A stainless steel gas permeation setup with an effective area of 8 cm² was used for the execution of permeation experiments.[42] A bubble flow meter was used to measure the flowrates of the both O_2 and N_2 gases at constant temperature and varying pressures *i.e.* 1, 2, 3, 4 and 5 bars. The permeability of the membrane was calculated by means of expression (1):

$$P = \frac{QL}{\Delta P A} \qquad (1)$$

where Q is the flow rate (ml min^{-1}), A and L are the area (m²) and thickness (m) of membrane and ΔP is the difference of pressure (bar) between feed pressure and permeate pressure.

Whereas the selectivity of membrane (a_{O_2/N_2}) for O_2 and N_2 was calculated by using the following expression:

$$a_{O_2/N_2} = \frac{P_{O_2}}{P_{N_2}} \qquad (2)$$

Results and discussions

Synthesis of Co_3O_4/GO nanocomposite

The demonstrated Co_3O_4/GO nanocomposite was synthesized *via* a simple and straightforward single step sonochemical reaction. In this, CoSalen (cobalt precursor) was subjected to produce the nanoparticles son the surface of GO by the *in situ* application of high intensity ultrasonic waves. The generation of high energy during ultrasonication due to the collapse of overgrown bubbles resulted the rise in temperature (~5000 K), which subsequently decomposed the CoSalen in to CoO and Co_3O_4 at around 780 K.[43] The GO then acted simultaneously as substrate for deposition of nanoparticles and as morphology template due to its surfactant properties.[44] Considering the aforesaid properties of GO, Pham V. Chuyen *et al.* reported the decoration of ZnO nanoparticles on the sheets of GO.[45] The functional groups on the edges and basal planes of the aqueous solution of GO are proposed to work as anchor sites to interact with Co_3O_4 NPs through electrostatic interactions and physisorption binding. Furthermore, the illustrated method also supports the homogeneity in the shape of generated nano sized particles as compared to other synthesis methods.[46] Lamya *et al.*[32] also reported the sonochemical synthesis of Co_3O_4 nanoparticles in the presence of [EMIM][BF$_4$] ionic liquid but the final product was subjected to calcination at 400 °C for 4 h. However, this step was not required in current method.

Fabrication and characterization of MMM

Surface morphology of Co_3O_4/GO nanocomposite and fabricated membranes was studied by using SEM analysis at different magnification scales. Fig. 1a corresponds to the surface morphology of graphene oxide which shows the 2D morphology of unstacked nanosheet with wrinkled and folded textures. Whereas, Fig. 1b corresponding to the morphology of Co_3O_4/GO nanocomposite. It can be clearly seen that Co_3O_4 nanoparticles are well deposited on the nanosheets of GO. Fig. 1c shows the images of fabricated membrane embedded with Co_3O_4/GO nanocomposite. Homogenous allocation of inorganic nanofiller in the polymer matrix and their effective interactions could be confirmed by considering these images of dense membranes. However, the surface of membranes indicates the generation of voids due to the free volume in the polymeric chains. The most probable reason for this is the
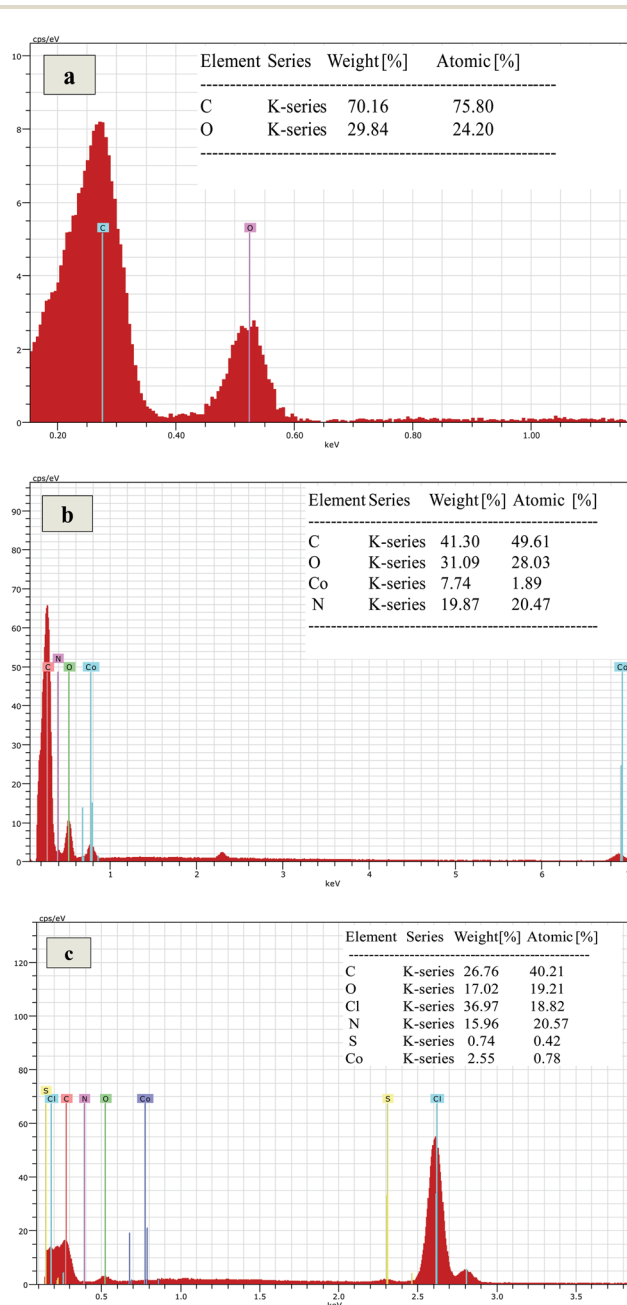

Fig. 2 EDS graph of: (a) GO, (b) Co_3O_4/GO nanocomposite, (c) Co_3O_4/GO nanocomposite embedded MMM.

interaction of polymer chains with inorganic nanofillers, which may enhance the free volume by disturbing the packing of the polymeric chains.[47]

The EDS analysis of synthesized membranes and Co_3O_4/GO nanocomposite was also conducted in order to confirm the fabrication of membranes with nanocomposite through elemental analysis and the obtained values for Kα and Lα were compared with the energy table. EDS graph of GO in Fig. 2a shows the two characteristic peaks of C and O. Fig. 2b shows the EDS graph of Co_3O_4/GO nanocomposite showing two peaks for Co at Lα and Kα with the values 0.78 and 6.98 respectively, along with the prominent peaks of C, N and O having the Kα values of 0.277, 0.392 and 0.525 respectively, which exactly matches to the energy table and confirms synthesis of Co_3O_4/GO nanocomposite. Fig. 2c corresponds to the EDS graph of membranes embedded with Co_3O_4/GO nanocomposite, which along with the peaks of S and Cl having the Kα values of 2.307 and 2.621 respectively, from membrane materials showing all the other characteristic peaks of Co_3O_4/GO nanocomposite. The weight% and atomic% of Co molecules decreased in MMM due to the interaction of molecules with polymeric precursors. Thus, confirming the successful fabrication of membranes with nanofiller.

The FTIR spectra of GO, CoSalen, Co_3O_4/GO nanocomposite and membrane embedded with Co_3O_4/GO nanocomposite are shown in Fig. 3. The appearance of stretching vibrations at 3401 cm^{-1}, 1648 cm^{-1}, and 1031 cm^{-1} indicate the presence of oxygen containing moieties such as hydroxyl, carboxyl, and epoxy groups in GO, respectively (Fig. 3a).[48] A sharp peak at 1624 cm^{-1} could be seen in IR spectrum of CoSalen (Fig. 3b)
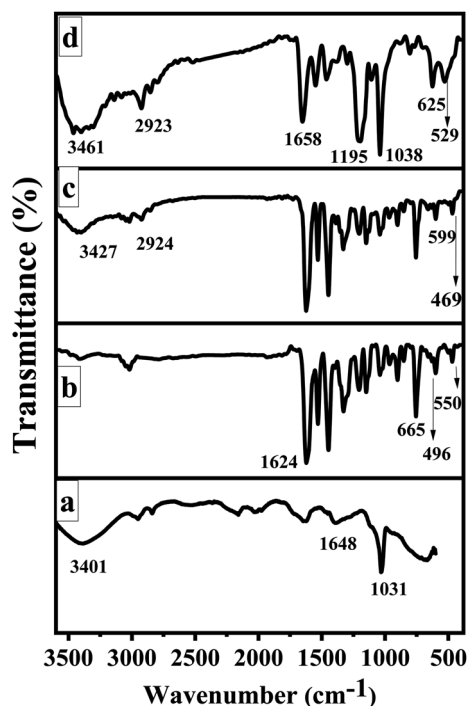
which can be readily assigned as the characteristic peak for Co ions-coordinated azomethane group (C=N) of salen. The vibration bands at 496 cm^{-1} and 550 cm^{-1} can be assigned to the Co–N and Co–O (phenolic) groups respectively. However, the stretching vibration mode of tetrahedrally coordinated Co^{2+}–O could be seen in the former peak at 665 cm^{-1}.[49,50] Fig. 3c exhibits all desired peak of Co_3O_4/GO nanocomposite. In this prominent peaks of OH group at 3427 cm^{-1} and CH stretching for alkyl groups at 2924 cm^{-1} due to GO. The bands at 599 cm^{-1} and 469 cm^{-1} originates from stretching vibration of metal–oxygen bond and are associated with Co–O vibrations in the octahedral and tetrahedral site of the lattice, demonstrating the presence of pure phase of Co_3O_4.[51] The occurrence of these bands in the region of lower wavenumber suggests the fine crystalline nature of materials in the nano range.[52] Fig. 3d represents the functionalities of membrane embedded with Co_3O_4/GO nanocomposite. The main peaks at 3461 cm^{-1} and 2923 cm^{-1} signify the presence of OH bond and C–H alkyl stretching, respectively. The peak at 1658 cm^{-1} is a typical carbonyl peak. Whereas the peaks at 1195 cm^{-1} and 1038 cm^{-1} are probably due to S=O groups of PAMPS. The peak at 625 cm^{-1} signifies the Cl stretching of PVC and at 529 cm^{-1} represents the metal–oxygen bond.

Raman spectroscopy is an extensively studied, non-destructive and powerful technique for the characterization of all members of carbon family. Mainly due to the observation of highly intense peaks for carbon–carbon double bonds and conjugated systems using this technique.[53] Raman spectra in Fig. 4a reflects the significant structural changes of GO during the synthesis. As compared to that of pristine graphite, the reduced size of sp^2 in-plane domains results the broadening and shifting of the D and G band in GO which could be observed at 1300 cm^{-1} and 1600 cm^{-1} respectively. Fig. 4b depicts the Raman spectrum of Co_3O_4/GO nanocomposite and dominated by one-phonon peaks attributed to the G- (~1600 cm^{-1}) and D-bands (~1310 cm^{-1}) of disordered sp^2 carbon, with an increase in D/G intensity compared to that of GO. This increment in intensity suggests the decrease in the average size of the sp^2
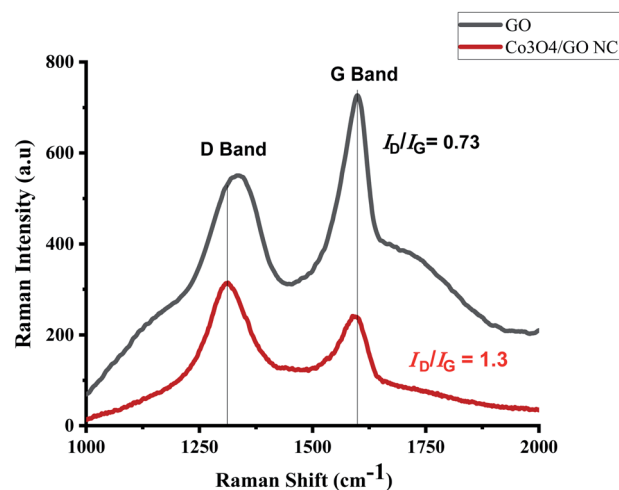

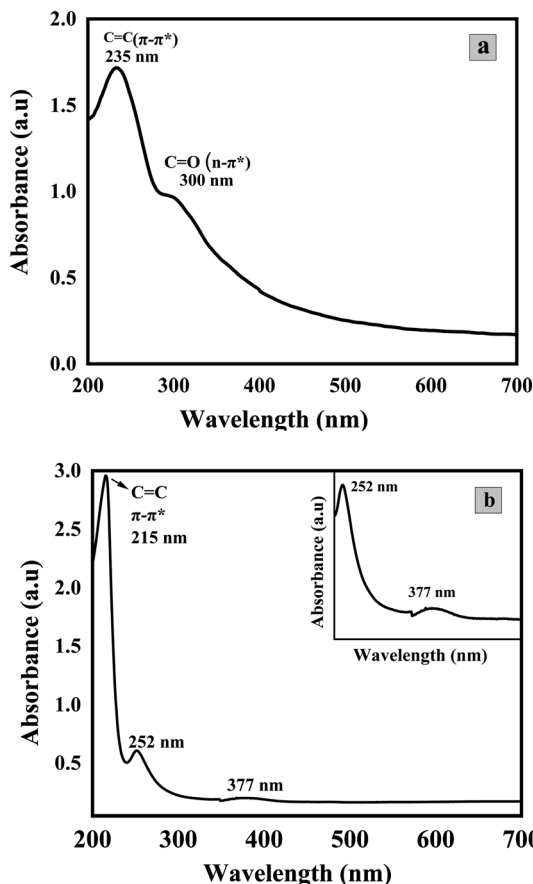Fig. 3 FTIR spectra of: (a) GO, (b) CoSalen, (c) Co_3O_4/GO nanocomposite, (d) Co_3O_4/GO nanocomposite embedded MMM.

Fig. 4 Raman spectroscopy analysis.

Fig. 5 UV-visible spectra of (a) GO and (b) Co_3O_4/GO Nanocomposite.

Fig. 6 X-ray diffraction pattern of: (a) GO, (b) Co_3O_4/GO nanocomposite.

domains and reduction in the crystallite size caused by a breakdown of the k-selection rule.[54]

Fig. 5 depicts the UV-visible absorption spectra of GO (a) and Co_3O_4/GO Nanocomposite (b). Two prominent peaks can be seen in the spectrum of GO in the range of 235 nm and at 300 nm possibly due to π-π* and n-π* transitions of C–C and C=O, respectively.[55] The absorption spectra of Co_3O_4/GO nanocomposite shows a prominent peak at 215 nm due to GO while two characteristic absorption bands of Co_3O_4 NPs could be seen at 252 nm and 377 nm.[56]

The quantitative estimation of degree of exfoliation and stacking of graphite and graphene oxide was perceived from XRD information. The modification of graphite into GO was assured by XRD pattern in Fig. 6a. A strong diffraction peak of GO was shifted to a lower angle of 001 plane at 11.8° with an interlayer spacing of 0.75 nm with respect to the sharp diffraction peak of pristine graphite at 26.7° on 002 plane with an interlayer spacing of 0.34 nm.[57] Suggesting the loose stacking of GO sheets due to the presence of oxygen-containing functionalities *e.g.*, –OH, C=O, –COOH and C–O–C between the layer of graphite.[58] The minor reflection at 26.5° and 44.9° suggests turbostratic disorder in graphene sheets.[59] The diffraction pattern of Co_3O_4/GO nanocomposite is represented in Fig. 6b. Peak at 11.8° is related to GO whereas at 19.99°, 32.2°, 37.88°
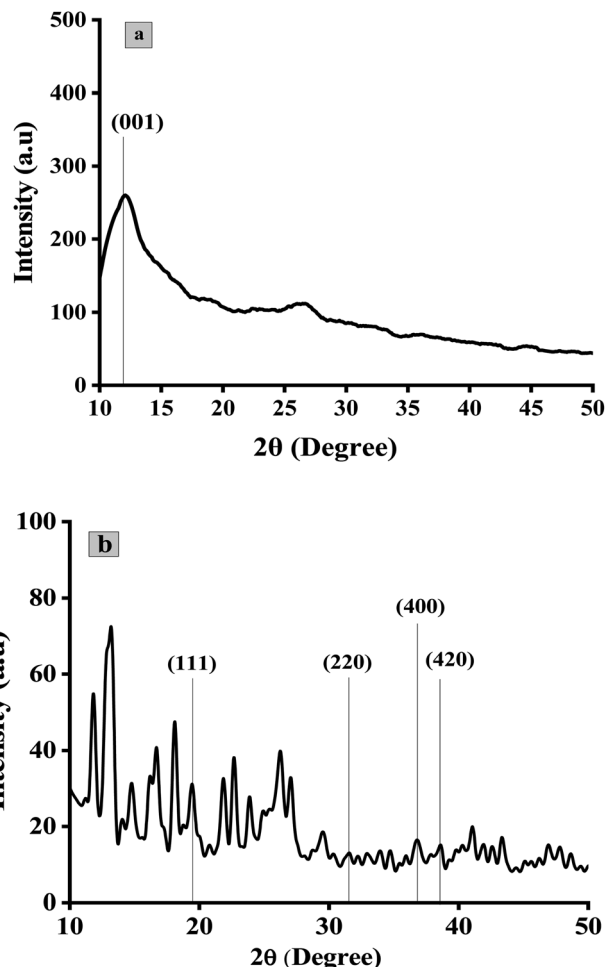
and 38.6° referent to (111), (220), (400) and (422) planes corresponding to Co_3O_4 nanoparticles.[51] The average size of particles obtained was approximately of 10 nm with SD of 3 nm calculated by Scherrer's equation.

Gas permeation results

Gas permeation experiments of different MMMs having the varying concentrations of Co_3O_4/GO nanocomposite were analyzed. The results were studied in aspects of effect of feed pressure on permeance of O_2 and N_2 and their separation factor based on the solubility and diffusivity of both gases in MMMs as compiled in Table 1. Fig. 7a and b shows that the permeance of gases increases by increasing the feed pressure from 1 to 4 bar; this could be explained in terms of dual-sorption model which elaborates the direct relation between the permeance of gases with the pressure due to the improved interaction between gas molecules and polymer chains.[60] Results also show that the permeance of O_2 is higher than that of N_2 at all pressures in all sample of membranes. This is possible due to the lower kinetic diameter of O_2 compared to N_2 (3.46 Å compared to 3.64 Å) and also due to the facilitated transport of O_2 by Co_3O_4/GO

Table 1 Gas permeation analysis results of different amount of Co_3O_4/GO nanocomposite embedded MMMs

Membrane samples	Pressure (bar)	Permeance (GPU)		Selectivity
		$P(O_2)$	$P(N_2)$	O_2/N_2
PVC/PAMPS	1	84.82 ± 0.47	82.12 ± 0.57	1.03 ± 0.45
	2	114.80 ± 0.21	109.34 ± 0.49	1.05 ± 0.68
	3	120.58 ± 0.36	114.13 ± 0.45	1.07 ± 0.49
	4	182.87 ± 0.27	170.84 ± 0.23	1.07 ± 0.50
PVC/PAMPS/Co_3O_4/GO nanocomposite (0.03% w/v)	1	17.49 ± 0.007	15.61 ± 0.04	1.12 ± 0.04
	2	90.78 ± 0.05	70.20 ± 0.73	1.29 ± 0.71
	3	139.34 ± 0.009	99.75 ± 0.27	1.40 ± 0.29
	4	238.97 ± 0.025	167.90 ± 0.28	1.42 ± 0.16
PVC/PAMPS/Co_3O_4/GO nanocomposite (0.04% w/v)	1	65.87 ± 0.80	51.19 ± 1.48	1.29 ± 0.81
	2	92.26 ± 1.25	66.93 ± 0.66	1.38 ± 1.91
	3	139.83 ± 0.07	90.00 ± 0.12	1.55 ± 0.11
	4	268.63 ± 0.05	141.64 ± 0.27	1.90 ± 0.22
PVC/PAMPS/Co_3O_4/GO nanocomposite (0.05% w/v)	1	431.68 ± 0.10	167.15 ± 0.50	2.58 ± 0.40
	2	787.88 ± 0.13	664.17 ± 0.09	1.19 ± 0.12
	3	1128.26 ± 0.05	963.15 ± 0.14	1.17 ± 0.11
	4	2175.09 ± 0.23	1702.25 ± 0.03	1.27 ± 0.25
PVC/PAMPS/Co_3O_4/GO nanocomposite (0.075% w/v)	1	430.60 ± 0.11	167.48 ± 0.16	2.57 ± 0.26
	2	751.06 ± 0.08	625.40 ± 0.04	1.20 ± 0.07
	3	1136.38 ± 0.05	957.31 ± 0.03	1.19 ± 0.03
	4	2116.30 ± 0.03	1702.25 ± 0.02	1.24 ± 0.02

nanocomposite, which speedups the transportation of oxygen molecules and increases the separation factor with respect to nitrogen molecules.[61] Azari Monsefi M. *et al.* reported the Pu-

PTH based polymeric membranes embedded with SiO_2 and TiO_2 Nanoparticles for O_2/N_2 separation. They obtained 10 barrers permeability for O_2 and separation factor of 2.5 with
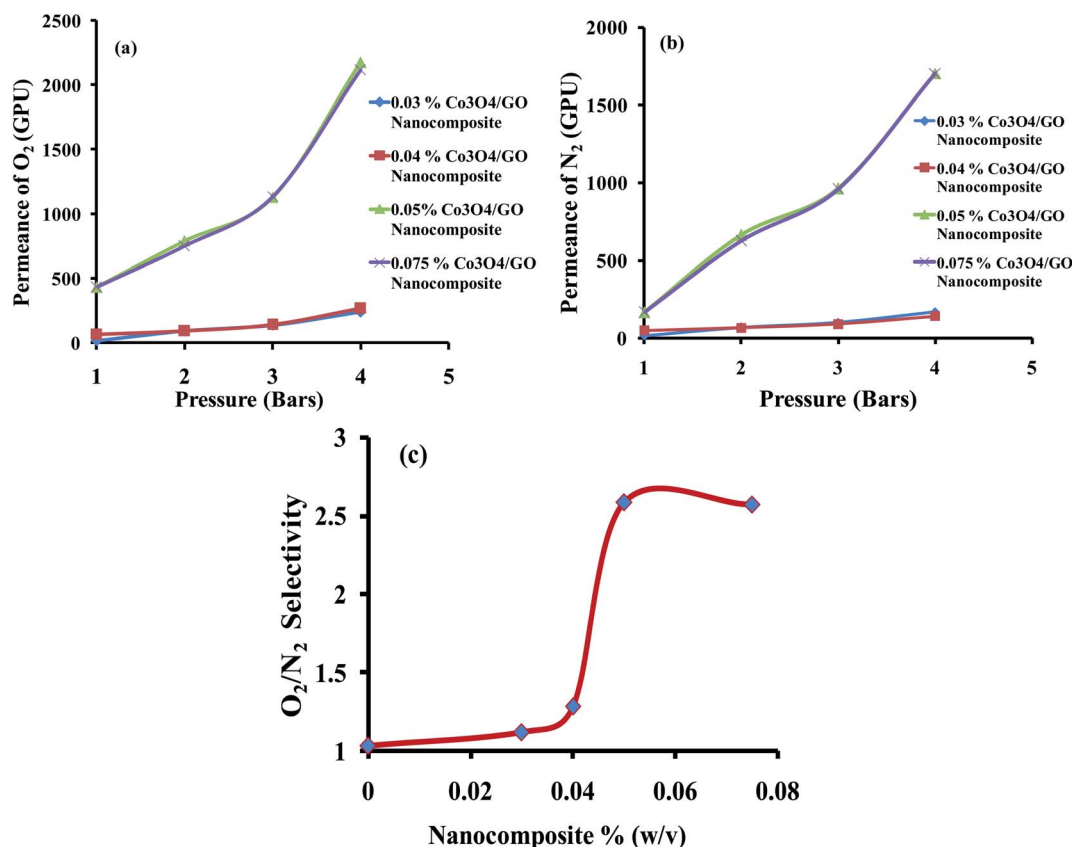

Fig. 7 Permeance of (a) O_2 (b) N_2 at different pressures for different concentrations of Co_3O_4/GO nanocomposite. (c) Selectivity of O_2/N_2 obtained for different concentrations of Co_3O_4/GO nanocomposite.

20% filler loading.[62] Another study reported the application of carbon nanotubes embedded in PDMS membrane for O_2/N_2 separation. Maximum selectivity achieved was 2.69 at 32.24 barrers.[63] In comparison, this study reports an excellent permeance of 432 GPU (18 735 barrers) for O_2 with 10% filler loading. The separation factor of membranes of varying composition for O_2/N_2 was improved as the concentration of filler was increased from 0.03% to 0.075%; see Table 1 and Fig. 7c. This is possibly due to Co_3O_4/GO nanocomposite; the enhanced linkages of cobalt oxide nanocomposite with oxygen ultimately help to facilitate the transportation of more O_2 through the membranes.[64] The best selectivity of 2.58 was obtained when MMM was loaded with 0.05% (w/v) of Co_3O_4/GO nanocomposite at pressure of 1 bar with permeance of 431.68 GPU. These results also reflect the cost effectiveness of the prepared MMMs as good results are obtained at 1 bar pressure. However, the concentrations less than 0.03% were also tried but they resulted in the uneven distribution of nanocomposite throughout the MMMs. Whereas, the MMMs embedded with more than 0.075% of nanocomposite were rupturing that may be attributed to overloading.

Conclusion

In this study, we have successfully demonstrated a facile, one-pot sonochemical route for synthesis of Co_3O_4/GO nanocomposite. Generally, Co_3O_4 NPs were synthesized at high temperature when CoSalen is used as precursor along with reducing agents. However, method used in this work is cost effective in terms of energy as similar results were obtained using sonochemical route of synthesis. The synthesized Co_3O_4 NC embedded MMMs appeared as efficient candidates for the separation of O_2/N_2 gases. It is observed that synthesized nanocomposite based MMMs can greatly incorporate to facilitate the transportation of O_2 molecules due to the efficient interaction of Co_3O_4/GO NC with O_2 molecules resulting in excellent permeance of 432 GPU for O_2 as compared to 167 GPU for N_2 at 1 bar. This fact was further furnished when different amounts of NC were loaded into MMMs. The permeance of MMMs was increased from 17.49 to 432 GPU for O_2 at 1 bar when amount of Co_3O_4/GO NC was raised from 0.03% to 0.05%. However, further increase in permeance was not observed with 0.075% of NC. Hence, the amount of nanocomposite relates directly to the selectivity of membranes. Furthermore, Co_3O_4/GO nanocomposite fabricated MMMs revealed excellent permeabilities which make them cost effective. Therefore, Co_3O_4/GO nanocomposite embedded PVC/PAMPS membranes are good candidates for cost effective separation of O_2/N_2.

Author contributions

Shahnila Shah: methodology, data curation, formal analysis, writing – original draft. Huma Shaikh: project administration, resources, conceptualization, methodology, writing – review and editing. Sarah Farrukh: formal analysis, investigation, supervision. Muhammad Imran Malik: formal analysis, supervision, investigation, review and editing. Zain un Nisa Mughal:

writing – review and editing. Shabana Bhagat: writing – review and editing.

Conflicts of interest

The authors declare that they have no competing interests that could influence the work reported in this paper.

Acknowledgements

References

1 A. Nikam, P. Bhagavatula and A. Kulkarni, *CrystEngComm*, 2018, **20**, 5091–5107.

2 M. S. Chavali and M. P. Nikolova, *SN Appl. Sci.*, 2019, **1**, 607.

3 K. Denishev, *J. Phys.: Conf. Ser.*, 2016, **764**, 012003.

4 L. Ji, in *Metal Oxides in Energy Technologies*, ed. Y. Wu, Elsevier, 2018, pp. 49–72, DOI: 10.1016/B978-0-12-811167-3.00003-1.

5 K. Uchino, in *Metal Oxides in Energy Technologies*, ed. Y. Wu, Elsevier, 2018, pp. 91–126, DOI: 10.1016/B978-0-12-811167-3.00005-5.

6 P. Wang, J. Wang, L. Fu, Y. Wu and T. van Ree, in *Metal Oxides in Energy Technologies*, ed. Y. Wu, Elsevier, pp. 17–47, 2018, DOI: 10.1016/B978-0-12-811167-3.00002-X.

7 I. A. Khan, F. Nasim, M. Choucair, S. Ullah, A. Badshah and M. A. Nadeem, *RSC Adv.*, 2016, **6**, 1129–1135.

8 C. S. Jincy and P. Meena, *Inorg. Chem. Commun.*, 2020, **120**, 108145.

9 Z. Ma, *Curr. Catal.*, 2014, **3**, 15–26.

10 X. H. Xia, J. Tu, J. Zhang, X. H. Huang, X. Wang, W. K. Zhang and H. Huang, *Electrochem. Commun.*, 2008, **10**, 1815–1818.

11 P. H. T. Ngamou, M. E. Ivanova, C. Herwartz, N. Lühmann, A. Besmehn, W. A. Meulenberg, J. Mayer and O. Guillon, *RSC Adv.*, 2015, **5**, 82717–82725.

12 E. Erdem, *Hybrid Mater.*, 2014, **1**, 62–70.

13 K. Latha, C. Prema and S. Sundar, *J. Nanosci. Nanotechnol.*, 2018, **4**, 475–477.

14 T. Ozkaya, A. Baykal, Y. Koseoglu and H. Kavas, *Cent. Eur. J. Chem.*, 2009, **7**, 410–414.

15 S. Sardjono and P. Puspitasari, *Synthesis and characterization of cobalt oxide nanoparticles using sol-gel method*, 2020.

16 D. Y. Kim, S. H. Ju, H. Koo, S. Hong and Y. Kang, *J. Alloys Compd.*, 2006, **417**, 254–258.

17 C. Young, J. Wang, J. Kim, Y. Sugahara, J. Henzie and Y. Yamauchi, *Chem. Mater.*, 2018, **30**, 3379–3386.

18 M. T. Makhlouf, B. M. Abu-Zied and T. H. Mansoure, *J. Nanopart.*, 2013, **2013**, 384350.

19 T. Senthamarai, V. G. Chandrashekhar, M. B. Gawande, N. V. Kalevaru, R. Zbořil, P. C. J. Kamer, R. V. Jagadeesh and M. Beller, *Chem. Sci.*, 2020, **11**, 2973–2981.

20 S. Mishra and S. Daniele, *Chem.–Eur. J.*, 2020, **26**, 9292–9303.

21 M. V. Landau, in *Handbook of Heterogeneous Catalysis*, 2008, pp. 119–160, DOI: 10.1002/9783527610044.hetcat0009.

22 T. G. Leighton, in *The Acoustic Bubble*, ed. T. G. Leighton, Academic Press, 1994, pp. 67–128, DOI: 10.1016/B978-0-12-441920-9.50007-9.

23 M. Ashokkumar and T. Mason, *Kirk-Othmer Encyclopedia of Chemical Technology*, 2007.

24 F. R. Young, *Cavitation*, World Scientific, 1999.

25 L. A. Crum, T. J. Mason, J. L. Reisse and K. S. Suslick, *Sonochemistry and sonoluminescence*, Springer Science & Business Media, 1998.

26 S. Naveenraj, S. Anandan, A. Kathiravan, R. Renganathan and M. Ashokkumar, *J. Pharm. Biomed. Anal.*, 2010, **53**, 804–810.

27 M. R. Hoffmann, I. Hua and R. Höchemer, *Ultrason. Sonochem.*, 1996, **3**, S163–S172.

28 T. Fujimoto, S.-y. Terauchi, H. Umehara, I. Kojima and W. Henderson, *Chem. Mater.*, 2001, **13**, 1057–1060.

29 R. Katoh, Y. Tasaka, E. Sekreta, M. Yumura, F. Ikazaki, Y. Kakudate and S. Fujiwara, *Ultrason. Sonochem.*, 1999, **6**, 185–187.

30 M. Bradley, M. Ashokkumar and F. Grieser, *J. Am. Chem. Soc.*, 2003, **125**, 525–529.

31 M. Ashokkumar and F. Grieser, *Rev. Chem. Eng.*, 1999, **15**, 41–83.

32 L. M. Al-Qirby, S. Radiman, C. W. Siong and A. M. Ali, *Ultrason. Sonochem.*, 2017, **38**, 640–651.

33 P. P. Goswami, H. A. Choudhury, S. Chakma and V. S. Moholkar, *Int. J. Chem. Eng.*, 2013, **2013**, 934234.

34 W. Gao, *Graphene Oxide – Reduction Recipes, Spectroscopy, and Applications*, 2015.

35 S. K. Alen, S. Nam and S. A. Dastgheib, *Int. J. Mol. Sci.*, 2019, **20**, 5609.

36 M. Jia, Y. Feng, S. Liu, J. Qiu and J. Yao, *J. Membr. Sci.*, 2017, **539**, 172–177.

37 S. A. S. C. Samarasinghe, C. Y. Chuah, W. Li, G. S. M. D. P. Sethunga, R. Wang and T.-H. Bae, *Sep. Purif. Technol.*, 2019, **223**, 133–141.

38 S. A. S. C. Samarasinghe, C. Y. Chuah, H. E. Karahan, G. S. M. D. P. Sethunga and T.-H. Bae, *Membranes*, 2020, **10**, 75.

39 W. S. Hummers and R. E. Offeman, *J. Am. Chem. Soc.*, 1958, **80**, 1339.

40 T. M. P. Deepika Das, *JoVE Science Education Database. Inorganic Chemistry. Synthesis of an Oxygen-Carrying Cobalt(II) Complex*, JoVE, Cambridge, MA, 2021.

41 S. Shah, H. Shaikh, S. Hafeez and M. I. Malik, *Pak. J. Ana. Environ. Chem.*, 2020, **21**, 10.

42 S. Hafeez, X. Fan, A. Hussain and C. F. Martín, *J. Environ. Sci.*, 2015, **35**, 163–171.

43 D. N. Kumar and B. S. Garg, *J. Therm. Anal. Calorim.*, 2002, **69**, 607–616.

44 L. J. Cote, J. Kim, V. C. Tung, J. Luo, F. Kim and J. Huang, *Pure Appl. Chem.*, 2010, **83**, 95–110.

45 C. V. Pham, S. Repp, R. Thomann, M. Krueger, S. Weber and E. Erdem, *Nanoscale*, 2016, **8**, 9682–9687.

46 M. Abbas, J. Zhang, K. Lin and J. Chen, *Ultrason. Sonochem.*, 2018, **42**, 271–282.

47 A. R. Moghadassi, Z. Rajabi, S. M. Hosseini and M. Mohammadi, *J. Ind. Eng. Chem.*, 2014, **20**, 1050–1060.

48 S. Thakur and N. Karak, *Carbon*, 2012, **50**, 5331–5339.

49 A. Khansari, M. Salavati-Niasari and S. Gholamrezaei, *Synth. React. Inorg., Met.-Org., Nano-Met. Chem.*, 2015, **45**, 1063–1068.

50 X. Yuan, F. Li, L. Wang and H. Luo, *Lat. Am. Appl. Res.*, 2007, **37**, 151–156.

51 M. Lima, C. Ferreira, Q. Rebelo, R. De Souza, R. Passos, E. A. G. Pineda and L. Pocrifka, *Mater. Res.*, 2018, **21**(2), e20170521.

52 J. Ma, S. Zhang, W. Liu and Y. Zhao, *J. Alloys Compd.*, 2010, **490**, 647–651.

53 K. N. Kudin, B. Ozbas, H. C. Schniepp, R. K. Prud'homme, I. A. Aksay and R. Car, *Nano Lett.*, 2008, **8**, 36–41.

54 F. Tuinstra and J. L. Koenig, *J. Chem. Phys.*, 1970, **53**, 1126–1130.

55 S. Farhadi, M. Javanmard and G. Nadri, *Acta Chim. Slov.*, 2016, **63**, 335–343.

56 L. M. Alrehaily, J. M. Joseph and J. C. Wren, *Phys. Chem. Chem. Phys.*, 2015, **17**, 24138–24150.

57 Z. Zhang, H. C. Schniepp and D. H. Adamson, *Carbon*, 2019, **154**, 510–521.

58 K. Zhang, L. L. Zhang, X. S. Zhao and J. Wu, *Chem. Mater.*, 2010, **22**, 1392–1401.

59 H. W. Wang, Z. A. Hu, Y. Q. Chang, Y. L. Chen, Z. Y. Zhang, Y. Y. Yang and H. Y. Wu, *Mater. Chem. Phys.*, 2011, **130**, 672–679.

60 W. J. Koros, D. R. Paul and A. A. Rocha, *J. Polym. Sci., Polym. Phys. Ed.*, 1976, **14**, 687–702.

61 W. Choi, P. Ingole, H. Li, S. Park, J. Kim, H.-K. Lee and I.-H. Baek, *Microchem. J.*, 2017, **132**, 36–42.

62 M. Azari, M. Sadeghi, M. Aroon and T. Matsuura, *J. Membr. Sci. Res.*, 2019, **5**, 33–43.

63 S. Kim, T. W. Pechar and E. Marand, *Desalination*, 2006, **192**, 330–339.

64 J. R. Potts, D. R. Dreyer, C. W. Bielawski and R. S. Ruoff, *Polymer*, 2011, **52**, 5–25.